EFFECTS OF HYDROSTATIC PRESSURE ON THE MECHANICAL BEHAVIOR OF BODY CENTERED CUBIC REFRACTORY METALS AND ALLOYS

(NASA Research Grant No. NsG-654) NGR-36-003-055

TECHNICAL REPORT

March 1969

prepared by

S. V. Radcliffe (Principal Investigator),

R. Daga and G. Das

Submitted to:

Office of Grants and Research Contracts

Attention: Code SC

National Aeronautics and Space Administration

Washington, D.C. 20546

DEPARTMENT OF METALLURGY AND MATERIALS SCIENCE

CASE WESTERN RESERVE UNIVERSITY

CLEVELAND, OHIO

ABSTRACT

The computed stress fields around spherical elastic discontinuities in an isotropic solid subjected to externally applied hydrostatic pressure have been compared with transmission electron microscopy observations of the pressure-induced development of dislocations in tungsten containing particles (thoria and hafnium carbide) or internal voids and in a model system of copper containing helium bubbles with the principal objective of elucidating the factors controlling the formation of such dislocations. For the tungsten, the computed value of the pressure required for dislocation nucleation is much below that observed experimentally. These observations of pressure-induced dislocations are interpreted in terms of additional stress concentrations associated with surface irregularities at the particles. In contrast to the tungsten, pressure-induced dislocations were observed around the helium bubbles in copper for a pressure (25 kilobars) in keeping with that predicted from the model. For both the tungsten and the copper systems, the development of pressure-induced dislocations depends strongly on the size of the elastic discontinuities. This result is shown to be in keeping with the interpretation of the mechanism of the development of pressure-induced dislocations as one of nucleation rather than multiplication of pre-existing dislocations. The results, together with the earlier studies of the influence of volume fraction of second phase carbide on pressurization effects in iron, have clarified considerably our understanding of the mechanisms involved and identified the controlling parameters. Furthermore, it is now possible to predict qualitatively the effects of pressurization for a given system and to make reasonable estimates of the magnitude of the associated property changes.

The flow and fracture characteristics of recrystallized arc-melted tungsten under tension have been determined at environmental pressures from one atmosphere up to 11 kilobars. Increase in pressure is found to retard the normally catastrophic failure and, above some 3 kilobars, macroscopic plastic yielding and work hardening occurs before fracture. While the yield stress remains essentially constant over the entire pressure range, the fracture stress increases significantly beyond 5 kilobars. Correspondingly, the fracture mode changes in that the proportion of intergranular to transgranular failure increases. The observed pressure dependence of the fracture characteristics points to serious deficiencies in current theory. The apparent importance of intergranular fracture has significance for the direction of future research on the factors controlling brittle fracture in tungsten under ambient conditions.

CONTENTS

I. INTRODUCTION

The principal objectives of the overall research program are (a) to investigate the pressure dependence of the flow and fracture behavior of tungsten in order to improve understanding and control of such behavior at both high pressure and under ambient conditions and (b) to examine the mechanism of pressure-induced generation of dislocations at elastic discontinuities and the relation between such dislocations and the associated changes in the early stages of plastic deformation. Three graduate students have been involved in the program - Mr. Das and Mr. Daga on the tungsten studies, and Mr. Trester on iron - with Professor S. V. Radcliffe as principal investigator. During the program, Mr. Trester was awarded a Master of Science degree, based in part on a thesis research conducted under the NASA Grant and took up an industrial research post. Mr. Das was awarded a Ph.D. degree, also involving a thesis based on the tungsten research and, after continuing with the program for a period on a post-doctoral appointment, has now taken a post in industry.

Four publications during the recent period arising from the research in the program are as follows:

- G. Das and S. V. Radcliffe; "Effects of Hydrostatic Pressure on the Mechanical Behavior of Tungsten"; J. Japan Inst. Metals, 334, 9 (1968).
- G. Das and S. V. Radcliffe; "A High Precision Microjet Technique for the Preparation of Electron-Transparent Foils in Thin Specimens" in Electron Microscopy, 1968. Tipographia Poliglotta, Rome 1968.

- G. Das and S. V. Radcliffe; "Internal Void Formation in Powder Metallurgy Tungsten". Trans. AIME, 2029,242,(1968).
- S. V. Radcliffe; "Influence of Grain Size on Pressurization Effects in Iron". Scripta Metallurgica, 59, 3, (1969).

Two further papers have been submitted for publication. Oral presentation of papers dealing with various aspects of the research were made at major meetings by P. Trester and G. Das at the Annual Meeting of The Metallurgical Society of AIME in New York, February 1968, and by S. V. Radcliffe at the Fourth Electron Microscopy Conference, Rome, Italy in September 1968. Mr. R. Daga is to present a paper at the Spring Meeting of the Metallurgical Society in Pittsburgh in May 1969.

During the present report period, the research carried out on mechanical behavior at pressure has been directed principally to determining the mechanical behavior of recrystallized arc-melted tungsten at pressures up to 11 kilobars and investigating the associated fracture modes by means of optical and scanning electron microscopy techniques. In the case of the pressurization phenomena, a more complete analysis than given previously[1] of the pressure-induced stress field at an elastic discontinuity has been used to develop a detailed understanding of both the conditions and mechanisms of the associated generation of dislocations. To assist in the development, a model system in which the elastic properties of the matrix and second phase are known and the matrix has a low flow stress, was selected to supplement the studies on tungsten and iron containing second-phase particles and reported previously[1]. For the model system, copper containing internal voids was selected and transmission electron microscopy was used to examine the effects of pressurization on the dislocation structure adjacent to these elastic discontinuities.

II. PRESSURIZATION PHENOMENA

In the previous work in this program, it was found that pressure-induced dislocations were developed adjacent to particles of thoria and hafnium carbide in a tungsten matrix as the result of pressurization to some 40 kilobars at room temperature. In the following, after describing the experimental procedures involved in the present work on the model system of copper containing internal helium-filled cavities, an analysis of the mechanisms of nucleation and multiplication of pressure-induced dislocations with respect to the earlier tungsten observations is given and finally, the results for the copper system are described and interpreted.

For the model system, high purity polycrystalline copper (99.999% Cu) in the form of annealed sheet (0.025 in. thick), prepared by rolling a zone-refined single crystal, was irradiated with 43 Mev alpha-particles in the cyclotron at Argonne National Laboratory, U. S. Atomic Energy Commission to a total dose of 1.4×10^{17} particles cm^{-2}. On subsequent annealing at 750^{o}C for one hour, helium bubbles were precipitated. These particular annealing conditions were selected to develop large bubbles, on the basis of previous studies of helium precipitation in copper[2,3,4]. Pressurizing up to 25 kilobars at room temperature was carried out on small specimens in a modified piston-cylinder apparatus of the Bridgman-Birch type. An equi-volume mixture of n-pentane and isopentane was used as the pressure fluid and the pressure was measured from the change in electrical resistance of a manganin wire gage within the pressure chamber. Thin foils for electron microscopy were prepared by a combination of high precision microjet dimpling and final bath polishing (using an extension of the technique developed earlier for the tungsten wires[5]) from thin strips (0.125" x 0.02" x .010") of the copper spark-cut to give a transverse section of the helium-rich layer.

A. Dislocation Nucleation

Pressure-induced dislocations were developed at 40 kilobars in tungsten at the particle/matrix interface regions[1] despite the fact that the calculated values of the corresponding maximum shear stress τ_{max} attainable in both the cases of thoria and hafnium carbide particles, G/225 and G/325, respectively, are still much below the nucleation stress for dislocation generation. These apparent discrepancies were discussed earlier[1] with respect to possible effects of departures from the simple, smooth-surfaced spherical particle assumed in the calculations and to the influence of residual thermal stresses around the particle. An additional and particularly significant characteristic will now be examined, namely that the development of pressure-induced dislocations around thoria or hafnium carbide particles in tungsten (as also for helium bubbles in copper, which will be discussed in detail later) is noticeably dependent on the size of the inclusion.

The continuum mechanics calculations[1] indicate that the value of the maximum shear stress attainable at the interface is independent of the size of the elastic discontinuity. This apparent paradox can be resolved if the details of the conditions necessary for the propagation of dislocations from the particle/matrix interface are taken into account. On this basis, a segment of dislocation is generated at the interface of a particle, independent of its size, when the pressure-induced shear stress reaches an appropriate value. However, the achievement of a full prismatic loop which can move away from the particle is strongly size dependent, as shown by the following argument.

It is apparent from Figure 1 that a dislocation segment (at L) of radius of curvature $a/\sqrt{2}$, where a is the radius of the discontinuity, nucleated on the circle of maximum shear stress marked II can glide under the action of shear stress parallel to its Burgers vector and the axis of the indicated glide cylinder (i.e., the shear stress circle marked I). The resulting development of a full prismatic loop thus occurs in accordance with the 'punching' mechanism suggested originally by Seitz in 1950 and modified for the thermal stress case by Jones and Mitchell[6]. The shear forces developed as a result of differential compression must support the line tension, F, of the dislocation, which can be written as:

$$F = \frac{Gb^2}{4\pi(1-\nu)} \left\{ \ln \frac{R}{b} + 1 \right\} \qquad (1)$$

where R is the radius of the loop and b is the Burgers vector. For small loops of the order of 500 Å (i.e. 200 b), F can be approximated as $Gb^2/2R$ and equated* with the work done by τ_{max} at L:

$$\tau_{max}\, b = \frac{Gb^2}{2R} \qquad (2)$$

---

*Recently and independently, a similar argument has been used for the case of the generation of glide dislocation loops by thermal stresses induced by quenching (7) to compute the critical particle size necessary to form the initial complete dislocation loop.

Equation 2 demonstrates that a pressure giving a shear stress which is sufficient to achieve the complete loop stage for a discontinuity of given diameter will be too small to reach this stage for a particle of smaller diameter. However, despite the qualitative agreement with observation, numerical calculations for the various tungsten cases based on this simpl, approach give critical sizes of discontinuity which are approximately one order of magnitude smaller than those at which dislocations were observed experimentally. In the case of copper, to be discussed later, closer quantitative agreement was obtained.

B. Dislocation Multiplication

Although the mechanism of dislocation generation due to stress concentrations at the surface irregularities of the particles appears feasible, the possibility of the induced stress at the particles causing multiplication of pre-existing interface dislocations cannot be overlooked. Thus, such a dislocation could operate as a Frank-Read source when the induced shear stress exceeds a critical value and give rise to prismatically punched dislocation loops or dislocation tangles. The stress to operate a source of one micron (i.e. the full particle diameter) would be as low as G/3650 in tungsten. Experimental measurements of proportional limits for high-purity tungsten single crystals[8] give flow stresses of a similar order of magnitude (5000 psi). The computed pressure to develop such relatively low stresses at the interface of elastic discontinuities is less than 10 kilobars.

For the voids in the PM tungsten matrix, the value of the maximum shear stress computed for 25 kb from the mathematical model is G/80, which is much higher than the value estimated abov for dislocation multiplication. However, no new dislocations were observed experimentally around voids after pressurization up to 25 kilobars. In the case of thoria and hafnium carbide particles, where the computed maximum values of the shear stress are G/360 and G/520, respectively at 25 kilobars, again no dislocation generation was observed after pressure cycling. From these arguments and observations it is deduced that pressure-induced dislocations in the tungsten are unlikely to be due to multiplication of pre-existing dislocations and that stress concentrations at the matrix-particle interface appear necessary to explain their formation.

C. <u>Copper Containing Helium-Filled Cavities</u>

The high energy (43 Mev) α-particles penetrated the copper to a depth of some 0.01 in. from the irradiated surface and came to rest in a narrow layer at that depth. The width of the layer or band of bubbles of He precipitated in this region on annealing was 0.006 in.

Previous electron microscopy studies of helium precipitation in irradiated copper(2,3,4) have been restricted, because of the difficulties of specimen preparation, to thin foils prepared parallel to the plane of the He-rich band. The high precision microjet thinning method developed for the present study has permitted the observation of the structural features across the entire width of the band.

As illustrated in Figure 2, the structure of the band in the irradiated and annealed copper consists of large spherical bubbles (1000 Å average diameter) in the outermost regions at both sides of the band and a dense population of very small bubbles (60-70 Å in diameter) in the interior of the band. The bubbles are generally free from dislocations, except for occasional interconnecting dislocations. In contrast, after pressurization to 25 kilobars, pressure-induced dislocations are visible in the matrix at many of the bubbles (Figure 3). Around the larger (500 - 1500 Å) bubbles, dislocations are seen as a dense "woolly" tangle somewhat similar to that reported for Fe_3C particles in iron(9). Some of the bubbles which have dislocations associated with them no longer have the spherical shapes seen in the annealed structure. Figure 3c illustrates well-developed prismatic dislocation loops which develop along 220 directions. In contrast to these features associated with the large bubbles, the smaller bubbles situated in the interior of the band appear unaffected by the pressurization. The minimum size of bubble that was observed to be effective in generating dislocations is 500 Å. In a few cases (see Figures 3a, 3b), bubbles of an average size less than 500 Å also appear non-spherical in shape, but without having dislocations visible around them even when examined carefully over a range of diffraction contrast conditions.

The above observations of dislocation generation under pressure are in keeping with the conditions calculated earlier[1]. The computed value of the maximum shear stress generated at the bubble-matrix interface at 25 kilobars is G/27, which is larger than the estimated critical stress for the nucleation of dislocations in copper. Moreover, the facts that the smaller bubbles (60 Å in diameter) appear insensitive to pressurization and the minimum size of the bubbles required for dislocation generation is about 500 Å are in keeping with the arguments presented earlier as to the influence of size. It must be noted that the critical pressure required to form these new dislocations was not determined experimentally, since pressurization was carried out at 25 kilobars only - a pressure selected because the value of the maximum shear stress calculated for this pressure approaches the nucleation stress for dislocations. However, although additional experiments at lower pressures would be needed to distinguish unequivocally between the operation of nucleation or multiplication mechanisms for the development of the pressure-induced dislocations, the latter mechanism is considered unlikely in view of the fact that dislocations associated with the bubbles were observed only rarely prior to pressurization.

While the present results appear to be first direct observations of dislocations induced around gas bubbles in a metal matrix by the application of external hydrostatic pressure, indirect experimental evidence for this type of localized plastic deformation has been reported by Miles and Gibbs[10] who noted permanent changes in the amplitude-dependent internal friction of air-melted polycrystalline aluminum after pressurization to 6 kilobars. The changes could be eliminated by annealing and did not occur in zone-refined aluminum. However, after re-melting in hydrogen the effect could be induced in the latter material also. It was deduced from these observations that the observed irreversible effects were due to the relaxation (Snoeck damping) of dislocations which had been formed at hydrogen-filled internal cavities when the specimens were subjected to high external pressure - i.e., an hypothesis in keeping with the experimental observations made here for copper. Additional evidence for pressure-induced plastic deformation at internal cavities was reported in 1964 by Norris[11] for lead iodide crystals (containing bubbles filled with iodine vapor) pressurized to 25 kilobars. Limited electron microscopy observations showed changes in contrast following pressurization which were interpreted as due to deformation of the gas bubbles and the formation of pressure-induced dislocations.

Direct observations of rows of prismatic dislocation loops in magnesium analogous to those developed here in copper on external pressurization have been observed by Lally and Partridge[12] for the inverse case of internal pressurization of hydrogen-filled cavities. The loops were observed in experiments at atmospheric pressure in which magnesium was heated and quenched in such a manner as to absorb hydrogen and then precipitate it in the form of small bubbles of high internal pressure. Using an extension of Eshelby's solution[13] for the shear stresses around a misfitting inclusion having the same elastic constants as the matrix, with inclusion and matrix being elastically isotropic, Lally and Partridge showed that shear stresses will develop in the matrix adjacent to the hydrogen-filled cavity. Comparison of their eqn. 1 for shear stress with that given here for the same problem indicates that the two approaches apparently agree only for the condition that $\nu = 1/3$. However, a recalculation based on the Eshelby model used by Lally and Partridge has indicated an error in their calculation and confirmed the correctness of the form of equation developed in the present work. Nevertheless, the hypothesis that the dislocation loops in magnesium are generated as the result of shear stress arising from the internal pressure remains valid and provides further support for the analysis presented in the present paper concerning similar phenomena developed by external pressure.

The stress field which arises around an internal discontinuity (cavity or inclusion) as a result of differential compression on pressure application is analogous to that which is developed due to differential thermal contraction during cooling. Accordingly, it might be expected that the nature of such pressure-induced dislocations would be similar to that of those induced thermally. Although a complete diffraction contrast analysis of pressure-induced dislocations has not yet been reported and has not proved possible in the present study, both the mechanism of loop formation and the nature of the loops have been examined for the thermal case[6,14]. For such loops at spherical glass particles in silver chloride, Jones and Mitchell[6] showed successive stages of formation to be nucleation of a dislocation segment in the region of maximum shear, followed by glide of the edge component away from the sphere along the surface of the glide cylinder and of the two screw components in opposite directions around the cylinder until they meet to form a full prismatic loop. Using transmission microscopy, Lawley and Meakin[14] showed that loops formed in a similar manner at carbide particles in molybdenum were interstitial in nature. The thermal and pressure cases are completely analogous when the discontinuity is a particle and the generation of interstitial loops would act in both cases to reduce the locally induced stresses by transporting material away from the particle-matrix interface. However, for an internal cavity (depending on the relative magnitudes of the internal and external pressures) the appropriate relaxation could require transport of vacancies away from the cavity, i.e., the formation of vacancy loops. The shape changes observed here for the cavities in copper (see Figure 5b) are in keeping with such a mechanism.

III. MECHANICAL BEHAVIOR OF TUNGSTEN AT HIGH-PRESSURE

In the previous study[1], the tensile behavior of powder metallurgy (PM) tungsten was examined over a range of hydrostatic pressure up to 11 kilobars at a constant strain rate (0.05 min^{-1}) and room temperature. In the case of the PM tungsten, it was established that only an increase in elastic strain to fracture was obtained up to 3 kilobars. Beyond this region, in the vicinity of 5 kb, discontinuous yielding followed by both plastic straining and work-hardening before fracture occurred and, with further increase in pressure to 8 and 11 kilobars, the yield drop persisted and the strain to fracture increased progressively. The low value of yield stress (96,000 psi) at room temperature obtained for the PM tungsten and the fact that no pressure-induced ductile-brittle transition phenomenon was observed within the range of pressure used were in marked contrast to the results obtained in more limited studies by earlier workers. Although the fracture stress of the powder metallurgy tungsten was observed to increase with pressure, the increase was not in keeping with the values predicted from recent theories of fracture of brittle solids at high pressure. The present research program, therefore, is aimed at investigating the tensile behavior of arc-melted tungsten under a range of hydrostatic pressures up to 11 kilobars under the identical conditions under which the powder metallurgy specimens were tested. The precise measurements made here of the pressure dependence of the fracture stress for well characterized recrystallized PM and arc-melted tungsten provides, for the first time, suitable data to permit the testing of theoretical ideas concerning the effects of pressure on fracture in a brittle bcc transition metal. Detailed consideration is given to this area and the results are discussed in the section following a brief description of some modifications and improvements in the apparatus.

The high pressure tensile apparatus and the 400/60 ton opposed ram hydrostatic press used to operate it has been described in detail in the previous reports[1,15]. During the present report period, several replacements and improvements have been introduced. A new lower piston for the high pressure chamber was made from stronger material than for the previous one (fully aged 300 CVM maraging alloy steel instead of hardened and tempered 4340 steel), which had failed. A new strain gage load cell (also of the maraging steel) was made to extend the load range up to 5,000 pounds. A modified high pressure seal for the electrical leads was developed to increase the seal life. The sealing arrangement differs from the one described in a previous report[1] principally in re-design of the conical plug. Six holes parallel to the surface are now drilled through the cone in place of 6 longitudinal grooves on its surface. The earlier piano steel wires have been replaced by six plastic coated copper wires (28 gage) sealed with epoxy cement and, as a result, the occasional problem of short circuiting due to contact between wire and the conical steel plug has been resolved. This lead system has been successfully used for pressures up to 11 kilobars.

Very recently, the cylinder which was in use has been replaced by a new high pressure cylinder made of maraging alloy steel. The previous cylinder had developed some enlargement of the bore and also plastic deformation at the window, making pressure sealing difficult. The different design of the new cylinder has reduced considerably the travel of the upper ram required to achieve a given pressure and up to 11 kilobars can be achieved with the glass windows in position.

A. Stress-Strain Behavior of Arc-Melted Tungsten as a Function of Pressure

High purity (99.999%, manufacturer's analysis) arc-melted tungsten was obtained in the form of as-swaged "surface ground" rod (0.31 in. diam.) from Universal Cyclops Company. Tensile specimens of the button-end type (overall length of specimen 1.75 in., gage length 0.6 in. and gage diameter (0.15 in.), Figure 4, were prepared from the rod by centerless grinding. The ground specimens were annealed in a tungsten crucible at 2200°C for one hour under vacuum in order to obtain a fully recrystallized structure. Possible surface damage from the machining was then removed by electro-polishing to reduce the diameter approximately 0.003 to 0.005". The electro-polishing was done at 10 volts in an electrolytic solution of 2% sodium hydroxide. The tensile testing on the specimens prepared in this way were carried out in the manner used previously[15] and covered the range from atmospheric pressure up to 11 kilobars at room temperature.

The tensile behavior observed in these tests is shown by the engineering stress-strain curves in Figure 5. The pressure dependence of the yield stress as a function of pressure is given in Figure 6. It is seen that, while arc-melted tungsten fails in a brittle manner in the elastic range at ambient pressure and temperature, the metal exhibits plastic yielding when the environmental pressure is increased to the vicinity of 3 kilobars. Further increases in pressure extend the range of plastic deformation to progressively higher stress and strain at fracture. The yield stress appears to be little affected by the increased pressure and it lies within $\pm$ 6,000 psi of a mean value of 75,000 psi. The small yield drop (discontinuous yielding) observed at 3 kilobars does not appear at higher pressures. Work hardening is observed in all specimens at pressures higher than 3 kilobars.

The tensile behavior of the arc-melted tungsten as a function of pressure resembles that of the PM tungsten with respect to the increase in fracture stress, but differs in three important factors.

Firstly, the yield stress and fracture stress both are lower for the arc melted tungsten, as shown in Figures 6 and 7. Secondly, effect of pressure on work hardening is larger. Thirdly, the plastic strain before fracture is much smaller in magnitude (see Figure 8). Previous measurements of the yield stress in compression for arc-melted tungsten at ambient pressure have shown that, for equal grain size, the arc-melted tungsten has lower strength than the PM tungsten(16). The lower strength of arc-melted tungsten observed here is in keeping with these results. While the yield stress of polycrystalline arc-melted tungsten at ambient pressure cannot be measured in tension at room temperature due to premature failure, single crystals exhibit yielding in tension, even at -196°C. A compilation of the published values of the tensile and compressive yield stresses for both single and polycrystalline arc melted tungsten over the ranges for which data is available has been made and the results are plotted in Figure 9. The average tensile yield stress of 75,000 psi measured in the present work at room temperature (and high pressure) is seen to be in quite good agreement with the extrapolated value of the temperature dependence of tensile yield stress for the polycrystalline material tested at ambient pressure.

Although the increase in fracture stress due to environmental pressure is approximately of similar magnitude in both PM and arc-melted tungsten, Figure 7, the fact that the arc-melted tungsten shows a higher work-hardening rate leads to its smaller improvement in ductility (strain to fracture). Other possible contributing factors are the larger grain size (0.5 mm, approximately ten times larger than that of the PM tungsten) and higher purity.

The observed pressure dependence of the fracture behavior is of particular significance and, accordingly, is discussed in more detail in the next section.

B. Fracture

The stress at fracture for the arc-melted tungsten as a function of pressure is shown in Figure 7. For comparison, the values obtained earlier for the powder metallurgy (PM) tungsten are also plotted in the same figure. Over the higher range of pressure, the fracture stress of both types of tungsten is seen to increase with increase in environmental pressure. However, the simple continuum mechanics fracture criterion of a critical "net tensile stress" (the difference between the applied axial tensile stress and the compressive hydrostatic stress) is clearly invalid for these materials because the increase in fracture stress does not appear to be linear and is considerably less than equal to the corresponding increase in hydrostatic compressive pressure. Furthermore the qualitative concept suggested by Bridgman[17] and more recently by Davidson et al[18] that the increase in fracture stress is simply equivalent to the corresponding increase of hydrostatic compressive stress is likewise invalid since this concept also predicts a direct proportionality between fracture stress and pressure. In a more sophisticated and different approach, Dower[20] has attempted a quantitative analysis of the ductile-brittle transition pressure found in zinc by examining the effect of hydrostatic compressive stress on crack propagation and assuming that nucleation of the crack is independent of pressure effects. He considered the principal parameters contributing to the energy of the crack as (a) the elastic energy of the stress field set up by the crack, (b) the surface energy of the crack, (c) the energy due to increase in volume on opening a crack under a hydrostatic stress field. Unfortunately, the resulting relationship involves terms for which numerical values are difficult to assess, so that it is not possible to apply the Dower equation generally to predict the pressure necessary to reduce the ductile-brittle transition to room temperature.

Very recently, Francois and Wilshaw[19] have attempted a more direct analysis of the influence of hydrostatic pressure on the fracture behavior of brittle polycrystalline metals by considering in detail the effects of pressure on the successive stages of crack nucleation, propagation across the grain and, finally, across the grain boundary. Crack nucleation by both the Stroh model (i.e., at grain boundary due to dislocation pileup, applicable to bcc metals) and the Stroh-Friedel model (i.e., due to splitting of an edge dislocation wall) was considered. Assuming that the cohesive strength (hence the surface energy) and the Peierls-Nabarro stress are independent of pressure and taking into consideration the orientation of the cracks with respect to the tensile axis, it was shown that catastrophic propagation of a crack (i.e., across both its grain and adjacent grains) to cause fracture is prevented when the normal stress at the crack is below a critical value, which is a function of the applied pressure. The Stroh model would be expected to be the more appropriate for tungsten and Figure 10 (taken from Fig. 8 in reference 19) illustrates the stability of cracks as a function of their orientation angle under the influence of superimposed axial stress σ, for the two cases of atmospheric pressure and high pressure. It is seen that for atmospheric pressure (Fig. 10a) the nucleation stress, σ_N, is larger for all angles of inclination of the cracks to the tensile axis than both the stress to propagate within the grain, σ_P, and that to cross into adjacent grains (the grain boundary propagation stress), σ_{GB}. As a consequence, fracture would take place at the minimum value of σ_N. Under these circumstances, a crack oriented at 45° to the tensile axis is the most probable one to cause fracture. In contrast, at high pressure (Fig. 10b) cracks may form and propagate across their grains, but only those having a favorable orientation, α_F, can propagate across grain boundaries in a transcrystalline manner - under the influence of the minimum applied stress for fracture, σ_F. This analysis leads to the relationship shown in Figure 11 for the pressure dependence of the fracture stress for particular sizes of dislocation pileup.

The experimental observations of the pressure dependence of fracture stress for arc-melted and PM tungsten are seen to be in marked disagreement with the relationship predicted by the Francois-Wilshaw analysis, in that the observed effects of pressure are much smaller. Furthermore, the observed characteristics of microcrack formation are different from those expected from the theory. Optical microscopy examination of the surfaces of the specimens tested up to 8 kilobars showed no evidence of microcracks, whereas those tested at 11 kilobars show numerous unpropagated microcracks, principally intergranular in character. These results suggest that at the lower pressure, crack nucleation is inhibited by the applied hydrostatic compression but that propagation occurs catastrophically once a crack does nucleate. In contrast, at the higher pressures increased plastic deformation occurs before final fracture and numerous intergranular cracks with a few transgranular cracks are found on the free surface of the specimen. Apparently, internal cracks form during initial plastic straining, but do not immediately lead to failure i.e., their rapid propagation is inhibited until further plastic strain occurs.

It should be noted that the increase in fracture stress before yielding at pressures below 3 kilobars may be, in one sense, only apparent. Namely, it is well known[21] that brittle fracture in tungsten at atmospheric pressure and temperature occurs over a wide range of stress values with a maximum stress for fracture equal to the macroscopic yield stress. The fracture stresses for PM and arc-melted tungsten under pressure shown in Figure 7 indicate that, up to a pressure of 70,000 psi ($\sim$5 kb), the fracture stress still lies within the range of the yield stress values. It is only beyond this pressure that the fracture stress clearly increases with increase in pressure.

In view of these several strong differences from the predicted behavior, some preliminary scanning electron microscopy observations of the fracture surfaces of the arc-melted tungsten specimens were undertaken in an attempt to clarify some indications obtained from optical microscopy that a change in the mode of fracture occurs at the higher pressures. Such a change might be responsible for the apparent disagreements. The scanning microscopy observations show that at lower pressures the specimens fracture mostly by transgranular cleavage with little intergranular separation, but that as the pressure is increased the proportion of intergranular separation also increases and transgranular cleavage is reduced. A typical fractured surface from a specimen tested at 3 kilobars is shown in Figure 12. The areas of "river pattern" characteristic of cleavage fracture are predominant on the fractured surface and the amount of intergranular separation is small. At 8 kilobars, the proportion of intergranular separation increases and at 11 kilobars, as shown in Figure 13, the proportion of intergranular separation is much larger than that of transgranular cleavage. These observations suggest that (a) only the <u>initiation</u> of cracks is inhibited in the lower range of pressure and the cracks, once formed, propagate catastrophically by transgranular cleavage. At higher pressures, both initiation and propagation are inhibited and the cracks which are initiated propagate mostly along the weaker path i.e., by intergranular separation, (b) the change in the fracture mode with pressure suggests that the plastic flow after yielding and the associated changes in substructure may play important roles in controlling the fracture behavior. Thus a modification in the F-W analysis which takes into account the plastic flow after yielding is necessary to establish a quantitative theoretical relation between fracture stress and environmental pressure.

It is of interest to note that a recently completed study in this Laboratory (E. Aladag, Ph.D. thesis, 1968) on the pressure dependence of the tensile stress-strain behavior of polycrystalline beryllium has also demonstrated the significance of intergranular failure in this normally semi-brittle material. In powder metallurgy beryllium, the intergranular mode predominated and could be suppressed only at the highest pressures. In ingot beryllium, in contrast, fracture occurred at all pressures by the transgranular mode. As for tungsten, considerable deviations from the predictions of the theoretical fracture model were observed. In the observations made at high pressure on these two different materials - the bcc metal tungsten and the hcp metal beryllium - it has thus been possible to inspect the processes of flow and fracture at room temperature and reveal important new information on the factors involved in these processes. In particular, the results point to the potential significance of fracture high pressure research directed to examining the nature of the grain boundary regions in relation to optimising resistance to fracture by restricting grain growth while avoiding grain boundary weakness.

IV. SUMMARY AND CONCLUSIONS

The present study has been concerned (a) to further elucidate the phenomena of pressurization as a basis for predicting its effects and possible utility and (b) to determine the pressure dependence of the tensile stress-strain behavior up to 11 kilobars in arc-melted tungsten, as a new means of examining the factors which determine the characteristically brittle behavior of recrystallized tungsten under ambient conditions. The principal results and conclusions are as follows:

A. Pressurization

1. In tungsten containing second-phase particles of thoria or hafnium carbide, the formation of pressure-induced dislocations at particles occurs for applied pressures which are lower than those predicted from the simple mathematical model. It is shown that additional stress concentrations from irregularities on the particle surfaces, possibly assisted by residual thermally-induced stresses, could account for these differences.

2. The magnitude of the applied pressure found to be necessary to develop dislocations at the particles precludes multiplication of preexisting dislocations as the relevant mechanism.

3. For copper containing helium-filled internal cavities, the magnitude of the externally applied pressure required to develop dislocations at the cavities is in reasonable agreement with that computed from the model.

4. The observed development of pressure-induced dislocations at cavities in copper supports earlier interpretations of pressure-induced permanent changes in the internal friction characteristics of aluminum

as being due to localized plastic-deformation at cavities.

5. For both tungsten and copper, the development of pressure-induced dislocations is observed to depend strongly on the size of the discontinuity. This result is shown to be in reasonable agreement - particularly for the case of cavities in copper - with computation of the size dependence of the energy necessary to nucleate a stable dislocation loop at a discontinuity.

B. Flow and Fracture of Arc-melted Tungsten

1. The tensile behavior at high pressure and room temperature differs substantially from that under ambient conditions. Increase in pressure retards catastrophic fracture and above some 3 kilobars macroscopic plastic yielding occurs prior to fracture. Further increase in pressure results in increased strain and work hardening before fracture occurs. However, even at the highest pressure used, 11 kilobars, the final fracture remains brittle.

2. The yield stress is essentially unaffected by increased environmental pressure and has a mean value of 75,000 psi with a range of $\pm$ 6000 psi. This mean value is in reasonable agreement with value obtained from extrapolation of high temperature tensile data from tests at atmospheric pressure.

3. The maximum fracture stress of the arc-melted tungsten is approximately constant up to 5 kb, beyond which it increases significantly.

4. The fracture mode changes with pressure in that the proportion of intergranular fracture increases relative to transgranular cleavage.

5. The general characteristics of the pressure dependence of the yield and fracture stresses are similar for brittle arc-melted and powder

metallurgy tungsten examined, although the stress levels are higher for the latter material.

6. The measured pressure dependence of fracture stress for tungsten differs in several important respects from the prediction of the most recent theory, the basis of which consequently must now be reassessed.

7. The observed prominence of the intergranular mode of fracture in tungsten points an area of potential importance for elucidating the factors leading to catastrophic fracture under ambient conditions.

REFERENCES

1. Radcliffe, S. V. and Das, G., Technical Report, December 1967 (NASA Grant No. NsG-654). Case Western Reserve University.

2. Barnes, R.S., Redding, G.B., and Cottrell, A.H., 1958, Phil. Mag. 3, 97.

3. Barnes, R.S., and Mazey, D.J., 1960, Phil. Mag. 5, 1247.

4. Ghosh, T.K., Beevers, C.J. and Barnes, R.S., 1960, J. Inst. Metals, 89, 125.

5. Das. G. and Radcliffe, S.V., 1968, in Electron Microscopy (Proc. Fourth European Conf. Rome, Sept. 1968) Vol.1 , p. 259 (Tip.Polig.Vaticana, Rome).

6. Jones, D.A. and Mitchell, J.W., 1958, Phil. Mag., 3, 1.

7. Gulden, M.G. and Nix, W.D., 1968, Phil. Mag., 18, 217.

8. Garfinkle, M., 1966, Trans AIME, 236, 1373.

9. Radcliffe, S.V. and Warlimont, H., 1964, Phys. Stat. Solidi, 7, 67.

10. Miles, M.H. and Gibbs, P., 1964, J. Appl. Phys., 35, 1941.

11. Norris, D.I.R., 1964, in Electron Microscopy, (Proc. Third European Conf. Prague, Sept. 1964) (Czech.Acad.Sci., Prague) Vol. A, 319.

12. Lally, J.S. and Partridge, P.G., 1966, Phil. Mag., 13, 9.

13. Eshelby, J.D., 1957, Proc. Roy. Soc., A241, 376.

14. Lawley, A. and Meakin, J.D., 1964, Phil. Mag. 10, 737.

15. Radcliffe, S.V., Das, G., and Trester, P., Technical Report June 1967 (NASA Grant No. NsG-654) Case Institute of Technology.

16. Witzke, W.R., Sutherland,E.C., and Watson, G.K., 1963 Tech. Note, NASA TND-1707.

17. Bridgman, P.W., 1952, studies in Large Plastic Flow and Fracture (McGraw-Hill Book Co., New York).

18. Davidson, T.E., Vy, J.G., and Lee, A.P., 1966, Acta Met. 14, 937.

19. Francois, D., and Wilshaw,T.R., 1968, J.Appl. Physics, 39, 4170.

20. Dower, R.J., 1967, Acta Met., 15, 497.

21. Hull, D., Beardmore, P., and Valentine, A.P., 1967, Plastic deformation of body-centered cubic metals, AFML TR66-369, Vol. II.

22. Aladag, E., Radcliffe, S.V., and Pugh, H.Ll.D. (to be published).

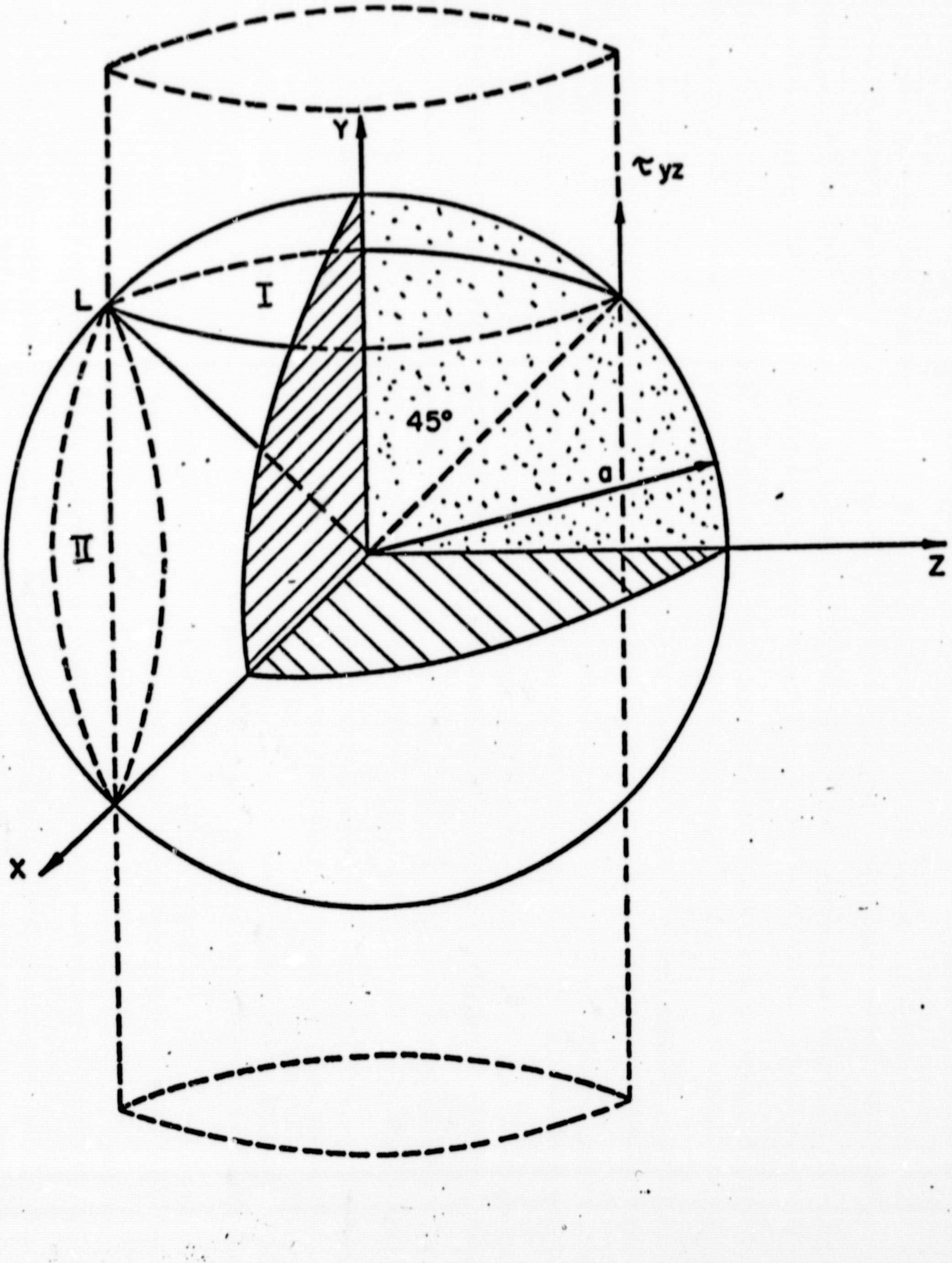

Fig. 1. Spherical "particle" of radius 'a' in a matrix subjected to external hydrostatic pressure. The intersection of the 90° cone with the surface of the sphere corresponds to a circle of maximum induced shear stress and defines the glide cylinder, shown by the dashed lines, for the induced dislocation loops.

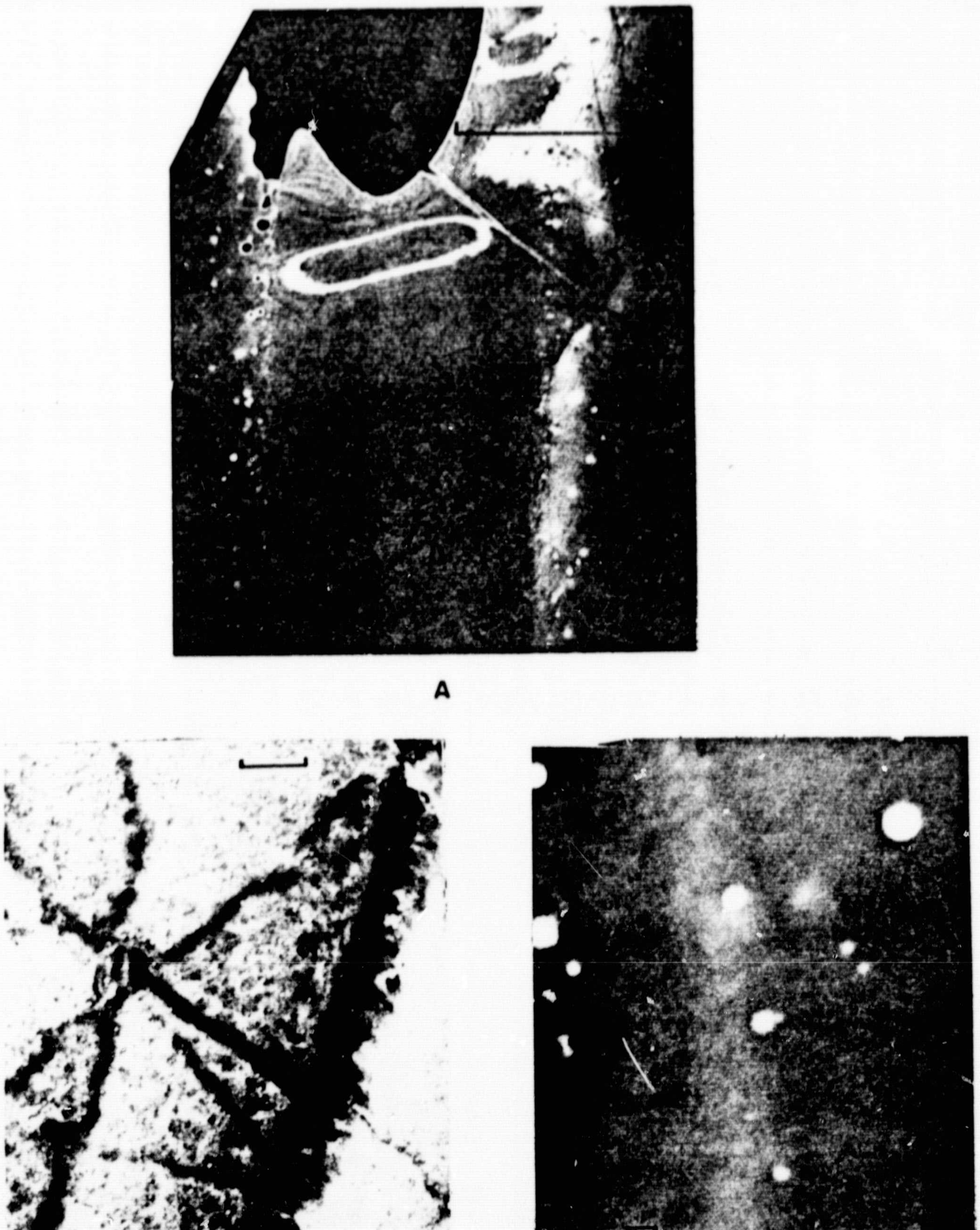

Fig. 2. Distribution of helium-filled bubbles in irradiated and annealed copper: (a) dark-field micrograph illustrating the changes in bubble structure across the full width of the helium-rich band; (b) large bubbles (average diameter 1000 Å) formed in the outermost regions of the band; (c) high density of small bubbles (average diameter 60 Å) formed within the band. The markers indicate 10 microns in (a) and 0.1 microns in (b) and (c).

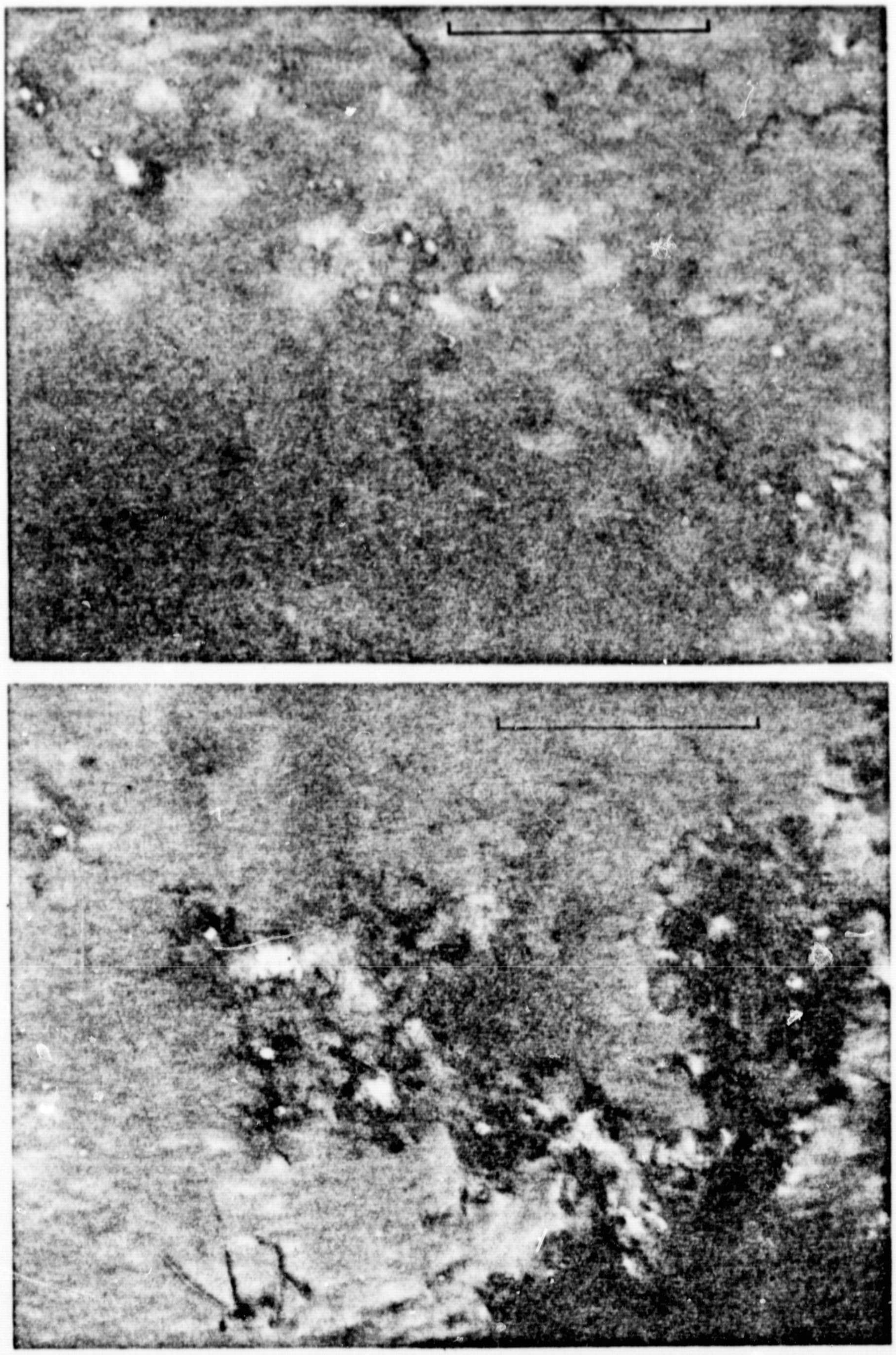

A

B

Fig. 3. Dislocations observed at helium-filled bubbles in copper following subjection to an external hydrostatic pressure of 25 kilobars: (a) Example of influence of bubble size on development of pressure-induced dislocations; (b) dense dislocation tangles observed at largest bubbles, together with examples of changes in the shape of the originally spherical bubbles; (c) simple array of prismatically punched loops developing along 220 direction from a helium bubble (marked A). The markers indicate 1 micron.

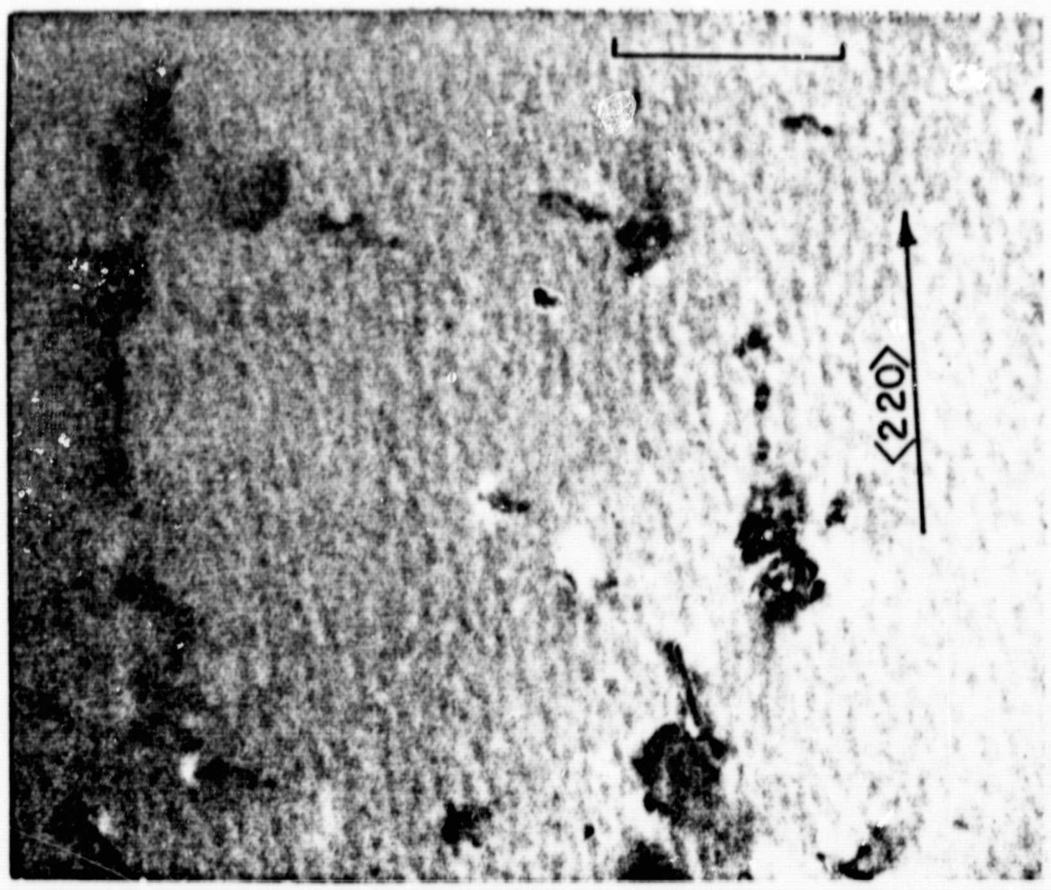

3(c)

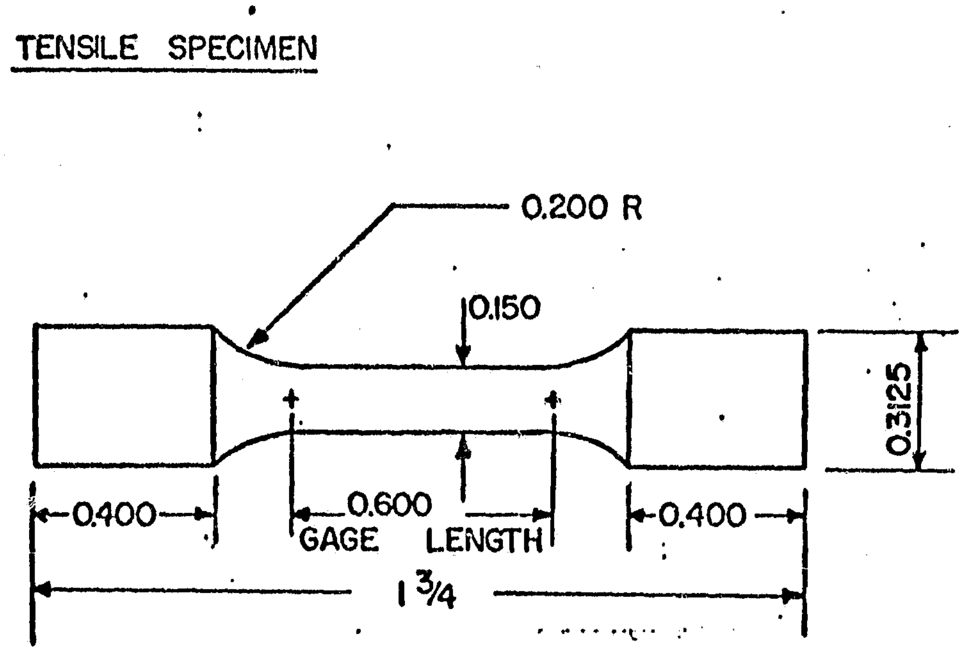
TENSILE SPECIMEN
0.200 R
0.150
0.3125
0.400
0.600
GAGE LENGTH
0.400
1 3/4

Fig. 4.

Tensile stress-strain curves for recrystallized arc-melted tungsten as a function of environmental pressure at room temperature.

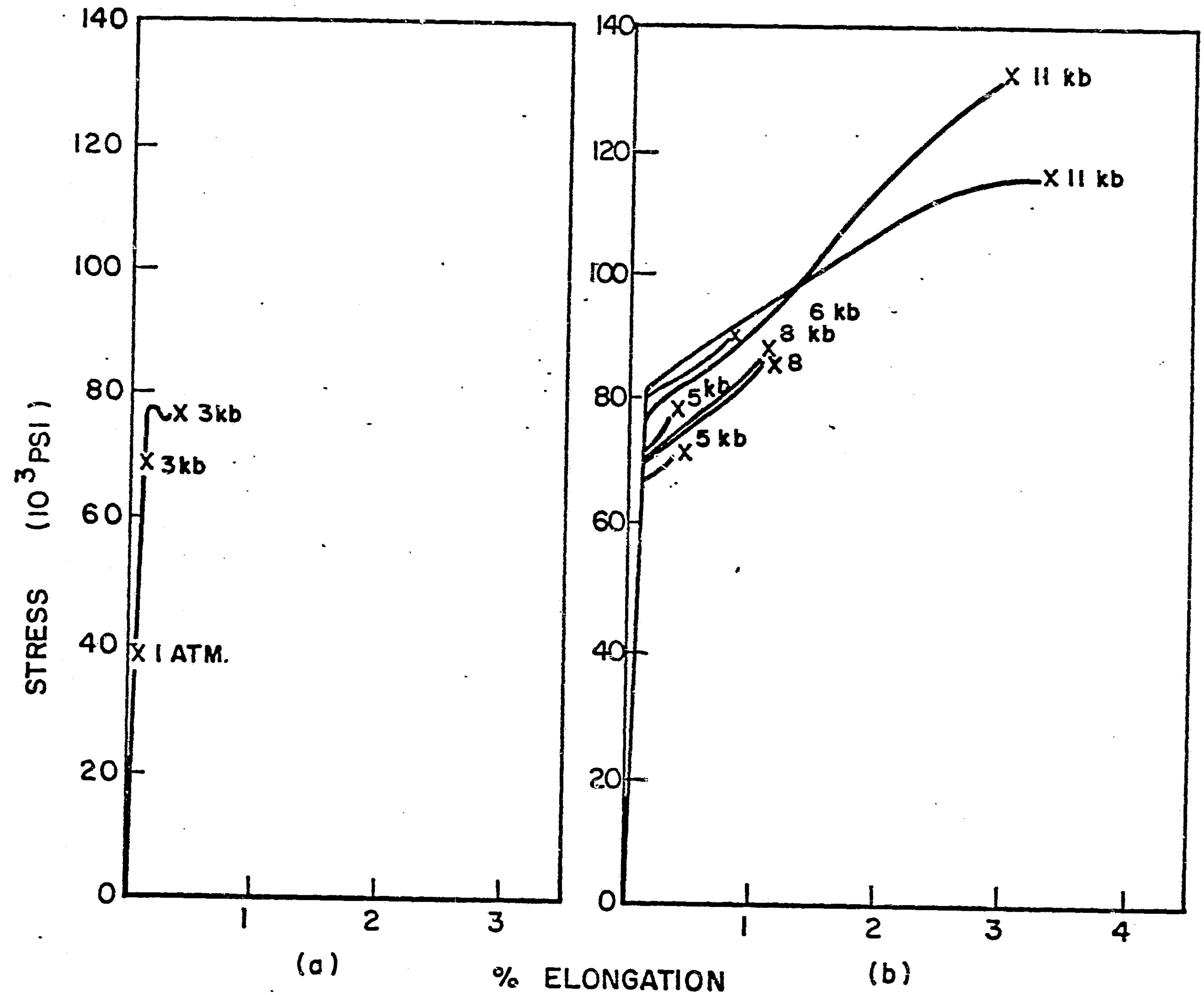

FIG. 5

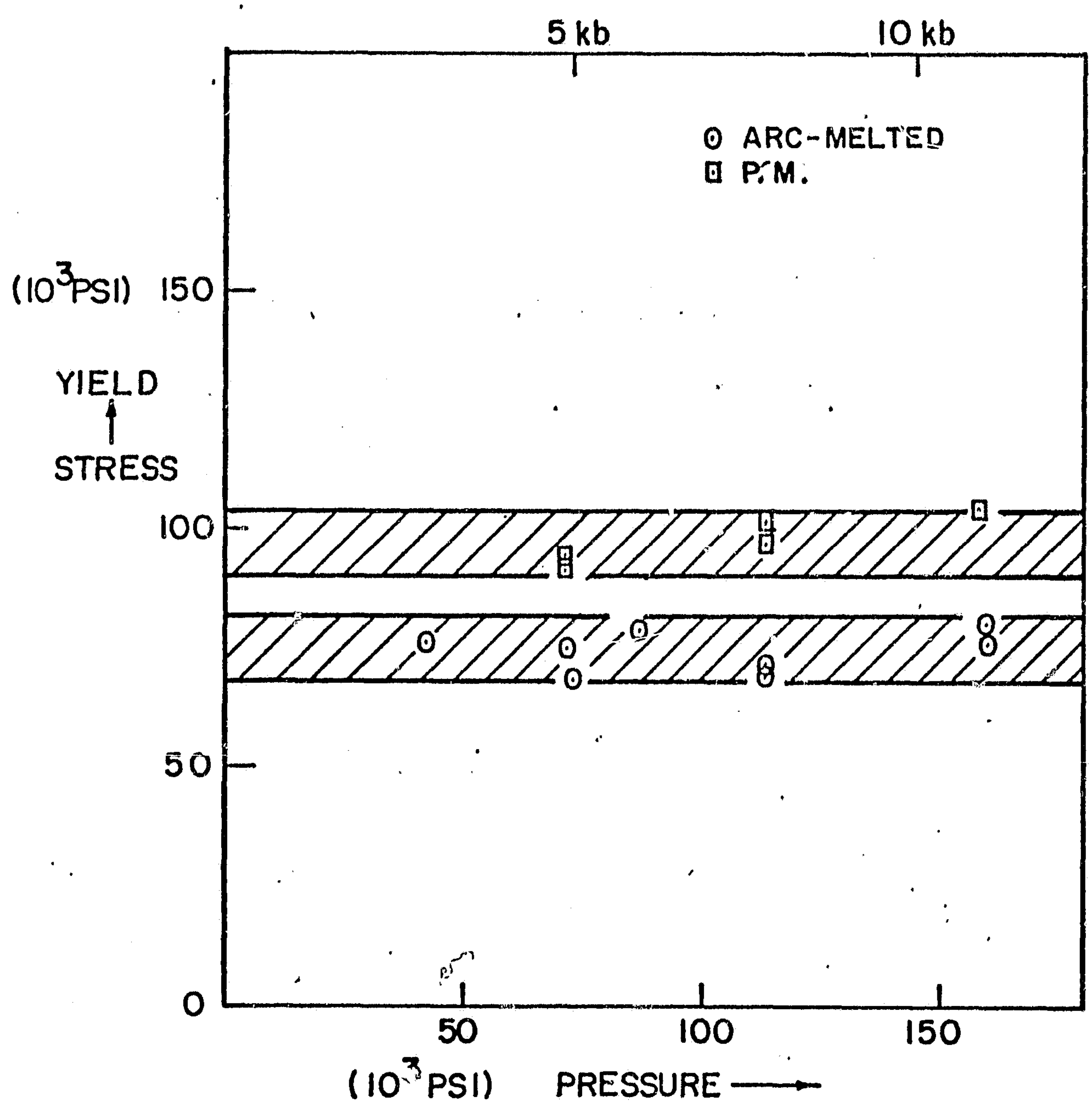

FIG. 6

Pressure dependence of yield stresses in tension of recrystallized PM and arc-melted tungsten.

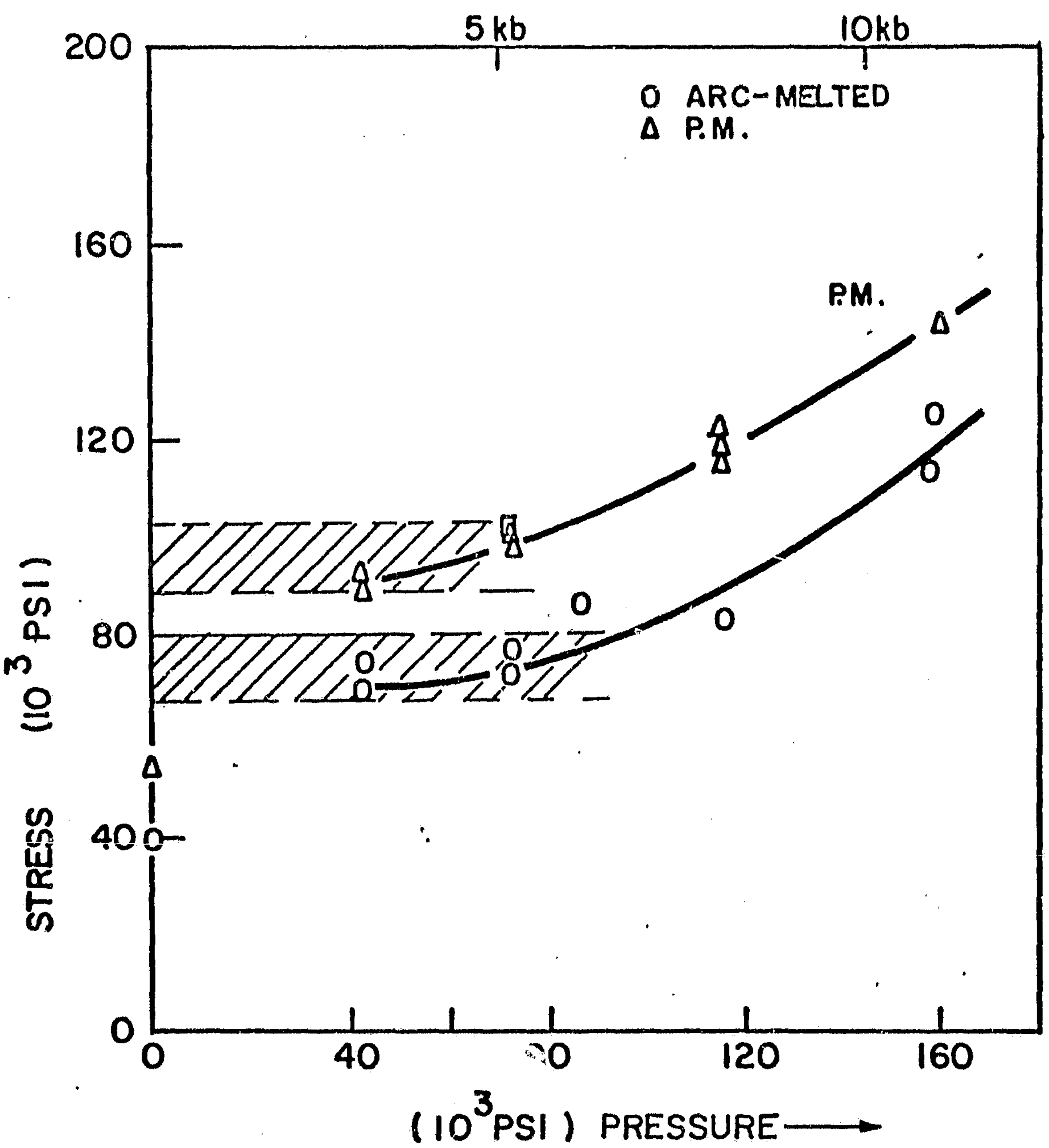

FIG. 7.

Pressure dependence of fracture stress in tension of recrystallized PM and arc-melted tungsten.

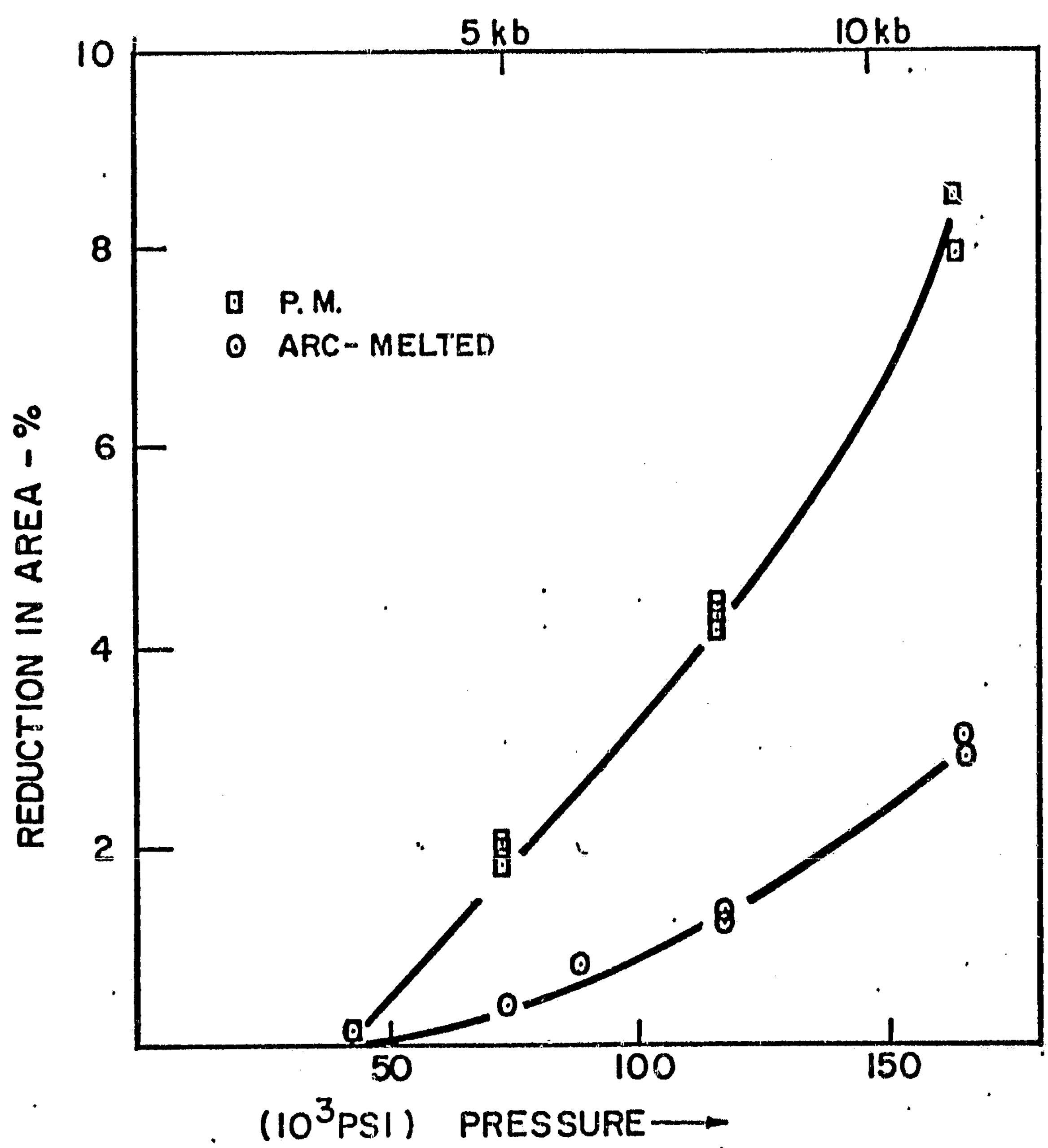

FIG. 8

Pressure dependence of the ductility (reduction in area) of recrystallized PM and arc-melted tungsten.

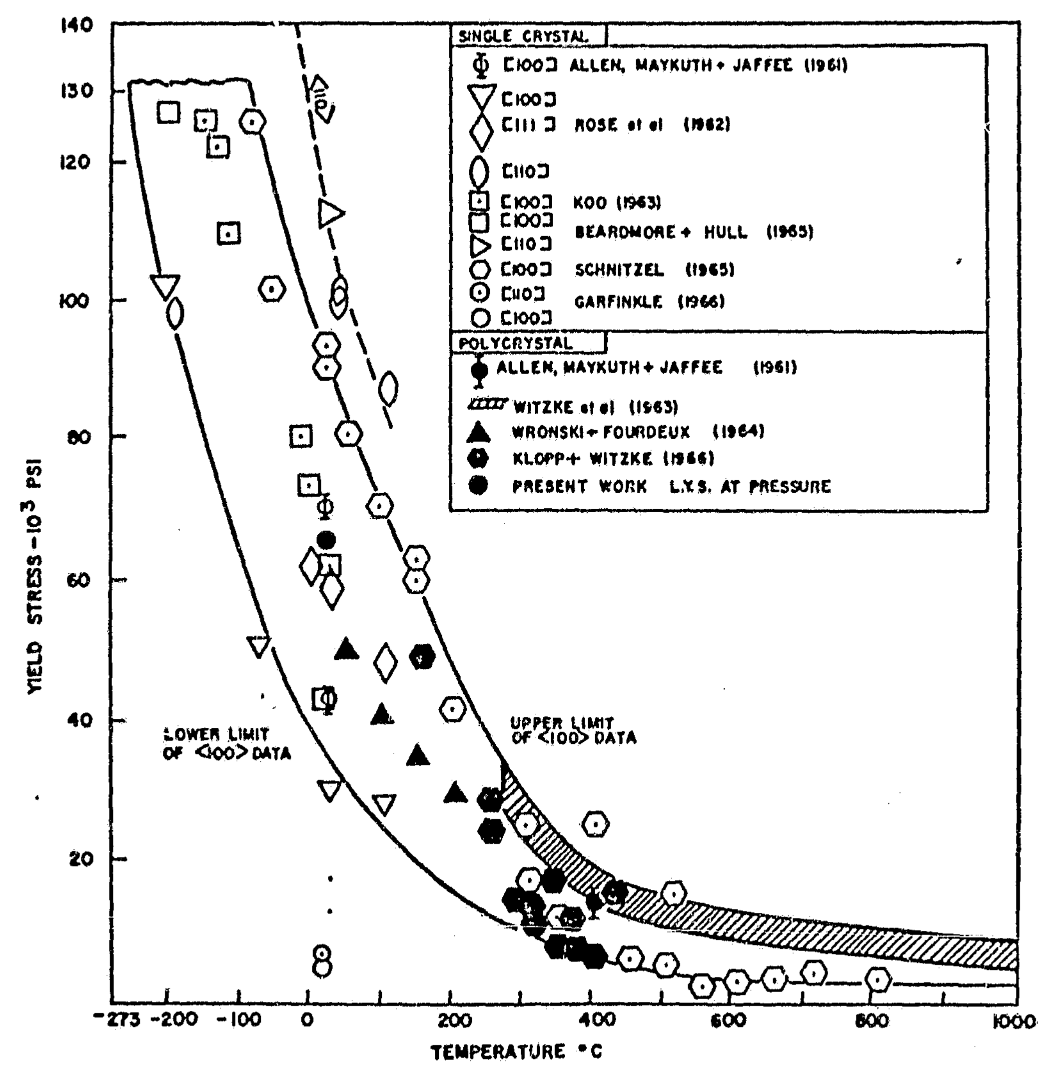

FIG. 9. COMPILATION OF REPORTED MEASUREMENT OF YIELD STRESS FOR MELTED (SINGLE CRYSTAL AND POLYCRYSTAL) TUNGSTEN AT ATMOSPHERIC PRESSURE. THE PLOT COMPARES THE DATA WITH THAT FOR ARC-MELTED TUNGSTEN DEFORMED IN TENSION UNDER HYDROSTATIC PRESSURE AT 25°C.

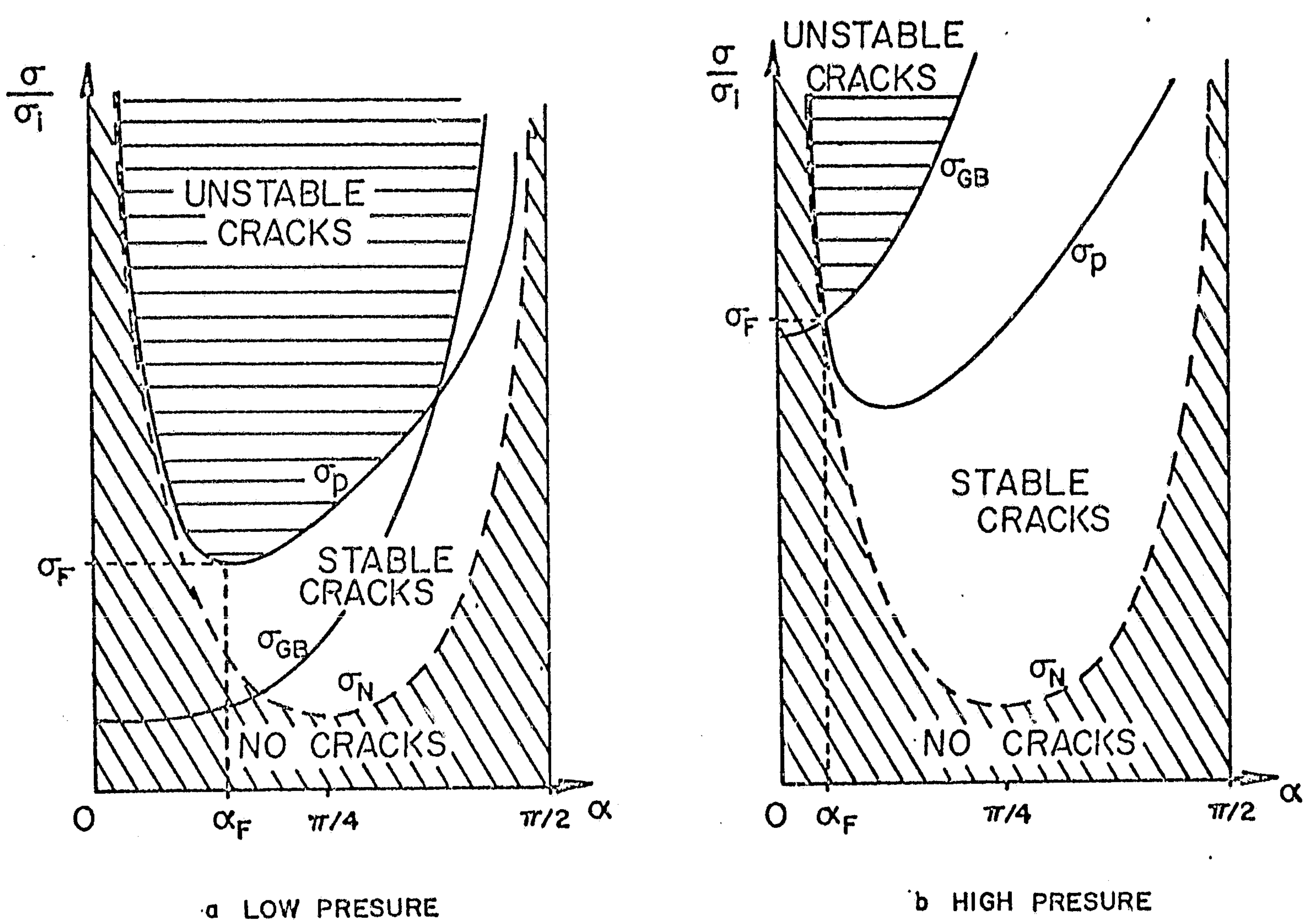

Fig. 10. The variation of the nucleation stress σ_N, the propagation stress σ_p and the grain boundary propagation stress σ_{GB} as a function of the orientation of the crack α for two pressures; (a) low pressure, (b) high pressure.

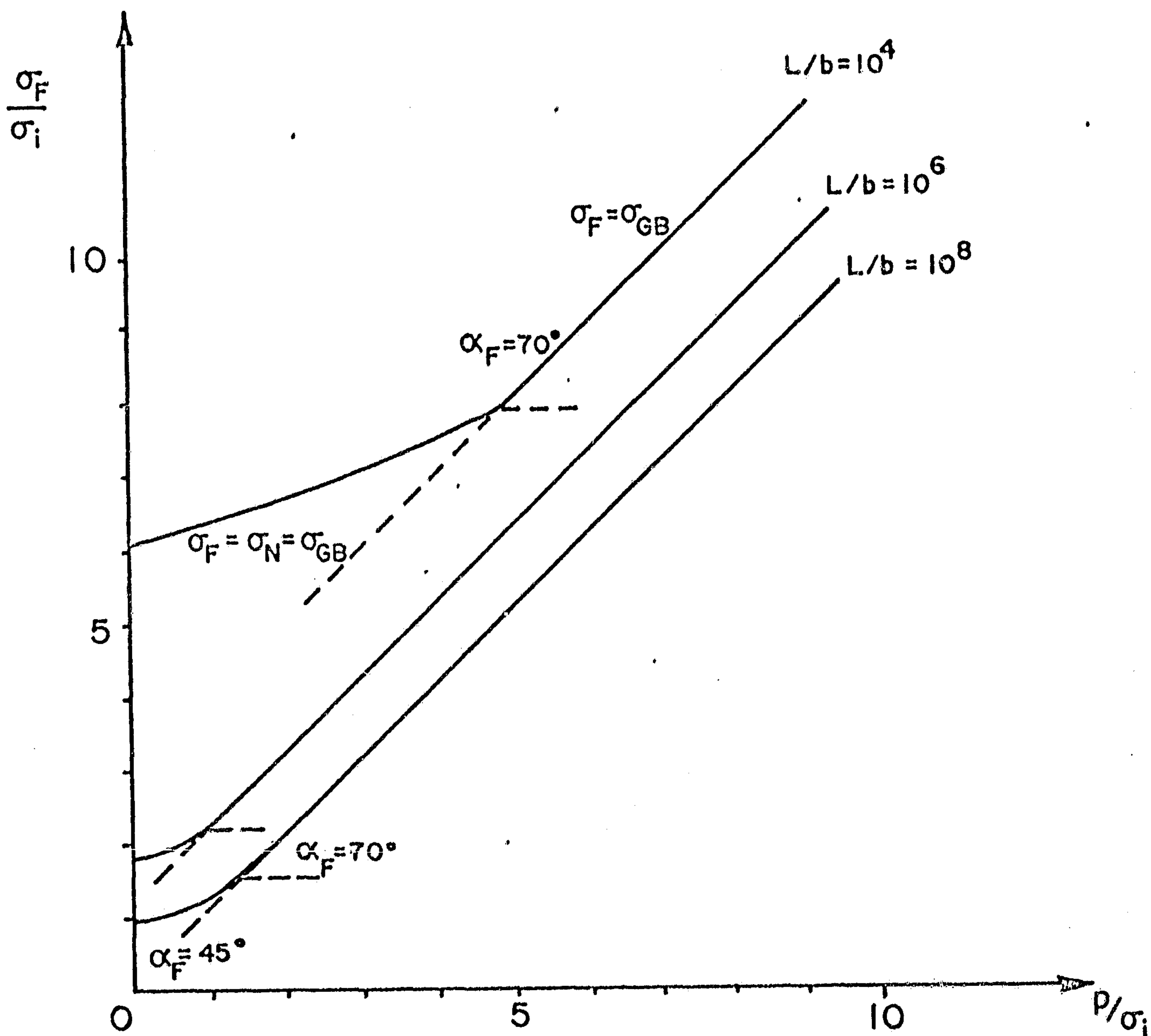

Fig. 11. The effect of hydrostatic pressure on the fracture stress for three different pileup sizes L/b.

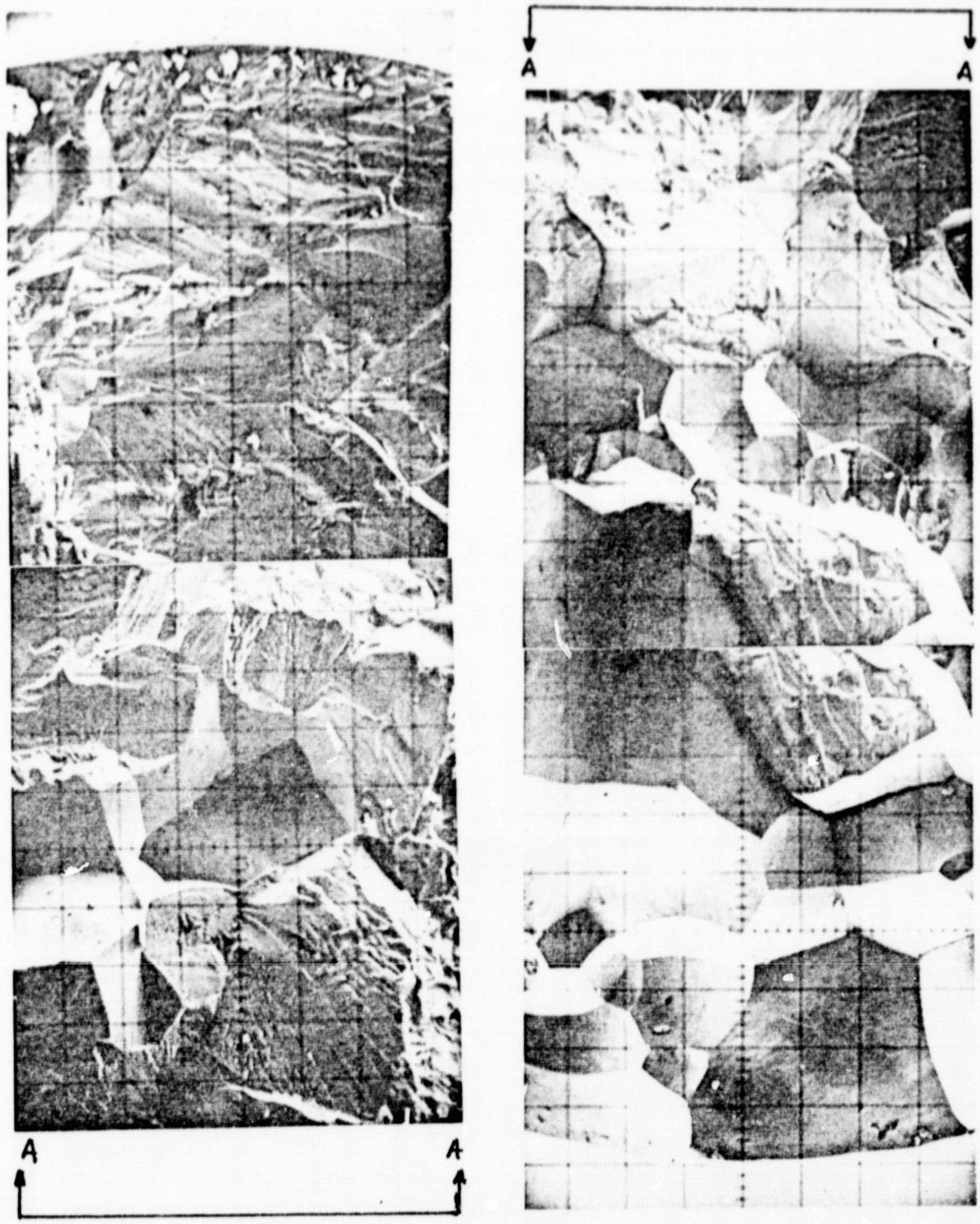

Fig. 13. Scanning electron-micrograph (100X) of specimen fractured under tension at 11 kb. Note region 'AA' is continuous along the diameter of the cross section of the specimen.